Jianpi Huoxue Decoction Ameliorates Alcoholic Liver Disease By Protecting Intestinal Barrier Function in Rats

Xin Wang
Institute of Liver Diseases, Shuguang Hospital affiliated to Shanghai University of Traditional Chinese Medicine
Dongsheng Yao
Institute of Liver Diseases, Shuguang Hospital affiliated to Shanghai University of Traditional Chinese Medicine
Lin Xu
Institute of Liver Diseases, Shuguang Hospital affiliated to Shanghai University of Traditional Chinese Medicine
Dongming Yan
Clinical Pharmacokinetics Laboratory, Shuguang Hospital affiliated to Shanghai University of Traditional Chinese Medicine
Yu Zhao
Shanghai Key Laboratory of Traditional Chinese Clinical Medicine
Jinghua Peng
Shanghai Key Laboratory of Traditional Chinese Clinical Medicine
Qilin Fu
Institute of Liver Diseases, Shuguang Hospital affiliated to Shanghai University of Traditional Chinese Medicine
Yiyang Hu
Key Laboratory of Liver and Kidney Diseases, Shanghai University of Traditional Chinese Medicine, Ministry of Education
Qin Feng (fengqin1227@163.com)
Key Laboratory of Liver and Kidney Diseases, Shanghai University of Traditional Chinese Medicine, Ministry of Education

---

Research Article

Keywords: alcoholic liver disease, Jianpi huoxue decoction, intestinal barrier function, intestinal permeability, tight junction

Posted Date: August 11th, 2021

DOI: https://doi.org/10.21203/rs.3.rs-745661/v1

Abstract

Background: Jianpi huoxue decoction (JHD), a Chinese herbal formula, is commonly applied in clinical practice for treatment of alcoholic liver disease (ALD) in China. Involvement of intestinal barrier function is increasingly recognized in the pathogenesis and progression of ALD. The aim of this study was to explore whether JHD on potentially protects intestinal barrier function in ALD rats.

Methods: Sprague-Dawley rats were randomly divided into three groups. Model (alcohol-fed) and JHD groups were fed Lieber-DeCarli liquid diets while rats in the control group were fed isocaloric maltose dextrin for six weeks. In the last three weeks of the respective diets, rats were intragastrically administrated JHD. Each rat received a gavage administration of lipopolysaccharide (LPS) before sacrifice. Gut leakage was evaluated by measuring LPS in the portal blood. Pathological changes in ileum tissue were observed by hematoxylin and eosin (H&E) staining. Ultrastructural changes of the intestinal tract were observed by transmission electron microscopy (TEM). The tight junction (TJ) proteins ZO-1 and occludin were assessed by western blot and immunofluorescence. Myosin light chain (MLC) phosphorylation, a key regulator of TJs, was also assessed by western blot.

Results: JHD administration attenuated Lieber-DeCarli liquid diet-induced hepatic steatosis and inflammation. Alcohol feeding increased portal vein plasma LPS levels in the model group. This deleterious effect was decreased in the JHD-treated group. Moreover, ileum tissue H&E staining demonstrated that JHD diminished intestinal inflammation. In addition, TEM indicated that JHD improved focal loosely packed microvilli. Furthermore, expression of ZO-1 and occludin decreased in the ileum tract of model rats. Finally, an increased level of p-MLC in the model group was also observed. JHD treatment reversed phosphorylation of MLC in the ileum.

Conclusions: The above results suggest that JHD has potential value in the prevention and treatment of ALD in rats; its mechanism of action may be closely related to its effect on improving intestinal barrier function and attenuating gut leakiness.

Background

Long-term drinking is a major cause of alcoholic liver disease (ALD), which can grow from alcoholic fatty liver to alcoholic steatohepatitis, liver cirrhosis, and hepatocellular carcinoma (HCC) [1, 2]. Approximately 3% of patients with alcoholic steatohepatitis develop cirrhosis annually [3]. Although the exact mechanisms of the pathogenesis of ALD are not well understood, a wealth of evidence indicates that excessive alcohol consumption can cause intestinal permeability to macromolecules and lead to an abnormal leakage of bacterial endotoxins [4-6]. This results in the release of proinflammatory mediators by macrophages and subsequent immunological and cytotoxic events, thereby inducing alcohol-induced liver injury [7, 8]. Therefore, the prevention of gut leakiness and ameliorating intestinal permeability may be central to the development of more effective prevention and treatment strategies for ALD [9].

Previous research has indicated that intestinal barrier function is integral function to gut leakiness [10, 11]. The intestinal barrier is the largest interface between external and internal environments in the human body [12, 13]. The intestinal barrier not only allows for the selective absorption of nutrients, but also limits host contact with pathogens and antigens [14]. It consists of a physical barrier, formed by the tight connection of tight junctions (TJs), which are necessary for intestinal barrier function [15]. Paracellular passive permeability through TJs regulates the absorption of many components in the intestine lumen [16]; however, this permeability barrier can be altered by means of a variety of physiological and pathological events that ultimately lead to an increase in permeability for bacteria, endotoxins, and other damaging compounds to enter the blood stream through the intestinal barrier [17].

Jianpi huoxue decoction (JHD), an effective traditional Chinese medicine (TCM) for long-term management of ALD, consists of eight Chinese herbs (*Curuma longa L.*, *Citrus aurantium L.*, *Atractylodes macrocephala Koidz.*, *Schisandra chinensis (turcz.) Baill.*, *Salvia miltiorrhiza Bge.*, *Paeonia lactiflora pall.*, *Alisma orientale (sam.) Juzep*, and *Pueraria lobata (willd.) Ohwi*). Previous research from our group has shown that JHD alleviates portal vein endotoxin leakage, suggesting a possible therapeutic use for ALD [18]. The potential mechanism of action, however, is unclear. Here, we adopted the Lieber-DeCarli liquid diet to study the hepatoprotective impact of JHD in rats. Subsequently, we investigated whether the mechanisms of JHD protection against alcoholic liver injury relate to preserving intestinal barrier function and limiting gut leakiness.

Methods

JHD preparation

The components of JHD are described in Table 1. To prepare JHD, *C. longa L.*, *C. aurantium L.*, and *A. macrocephala Koidz*. were distilled for 1–2 h with 60% ethanol three times. The ethanol was filtered and recovered. *S. chinensis (turcz.) Baill.* was extracted twice with 70% ethanol, and the ethanol was filtered and recovered. *S. miltiorrhiza Bge.*, *P. lactiflora pall.*, *A. orientale (sam.) Juzep*, and *P. lobata (willd.) Ohwi.* were extracted with water, and the filtrate was refrigerated and stored for later use. JHD was prepared in the Science and Technology Center of Shanghai University of Traditional Chinese Medicine. The concentration of the crude drug was 0.9 g/mL.

Ultra-high performance liquid chromatography-mass spectrometry (UHPLC-MS) analysis of JHD

JHD index compounds (puerarin, paeoniflorin, naringin, curcumin, atractylolide, schisandrin a, alisol 23b, and tanshinone) were analyzed using UHPLC-MS. The chromatography method was established on an ultra-fast liquid chromatography (UFLC) system (SHIMADZU, Kyoto, Japan) with an Agilent Eclipse XDB-C18 (4.6.150 mm, 5 μm; Santa Clara, CA, USA) analytical column for chromatographic separation. Mass spectrometric detection was carried out on a 4000 QTRAP (AB SCIEX, Framingham, MA, USA) equipped with an electrospray ionization source. The analysis was performed with a UHPLC-Q/Exactive system (Thermo Fisher Scientific, San Jose, CA, USA) equipped with a quaternary gradient pump, autosampler,

and high-resolution mass spectrometry detector. Puerarin, paeoniflorin, naringin, curcumin and atractylolide were analyzed in ESI- mode, schisandrin a, alisol 23b, and tanshinone were analyzed in ESI+ mode.

Animals

Male Sprague-Dawley (SD) rats (n = 30; 10 rats per group) weighing 130–160 g were acquired from Shanghai Bikai Laboratory (Shanghai, China). All animal testing protocols were approved by the Animal Experimental Ethics Committee of Shanghai University of Traditional Chinese Medicine. All rats were kept in a controlled environment at room temperature (25 °C) and for a 12 h light/dark cycle. After 7 d of adapting to laboratory conditions, rats were randomly divided into three groups with each group housed in its own cage.

SD rats were pair-fed a modified Lieber-DeCarli liquid diet (Tables 2 and 3) [19] containing alcohol (model group, n =10; JHD group, n =10) or isocaloric maltose dextrin (control group, n = 10) for six weeks. After three weeks on the respective diets, rats were administrated JHD intragastrically for three weeks. Rats in the JHD group were given JHD. Rats in the control and model groups received equal volumes of double-distilled water. At the end of the experiment, rats were orally administered 10 mg/kg LPS. After 3.5 h, rats were sacrificed and the plasma, liver, and intestinal tissues were collected.

Biochemical assays

The levels of alanine aminotransferase (ALT), aspartate transaminase (AST), and alkaline phosphatase (AKP) were measured using corresponding commercial test kits (Nanjing Jianchen Bioengineering Institute, Nanjing, China) according to the manufacturer’s protocols and in accordance with the manufacturer's agreement. Liver tissue (100 mg) was homogenized in 1.5 mL of 1:1 ethanol:acetone (v/v). The liver tissue triglyceride (TG) levels were determined using TG quantification kits (Dongou Bioengineering, Zhejiang, China).

Histopathology

In order to study pathological changes, liver and ileum tissues were fixed in 10% neutral formalin for 48 h. Then, the tissues were embedded in paraffin and sectioned continuously (4 meters thick). The slices were placed on glass slides and stained with hematoxylin and eosin (H&E; Nanjing Jianchen Institute of Bio Engineering, Inc.) and examined under a light microscope (Olympus Medical Systems, Tokyo, Japan). Analyses of liver pathological adjustments were based totally on the percentage of inflammation, necrosis (0 points, 0 foci; 1 point, < 2 foci; 2 points, 2–4 foci; 3 points, > 4 foci; per 200× field), and steatosis (0 points, < 5%; 1 point, 6–33%; 2 points, 34–66%; 3 points, > 66%), which were independently assessed by three examiners [20]. Ileum injury was evaluated by "Chiu" scoring method [21].

Transmission electron microscopy

A small section of the ileum tissue was fixed for at least 4 h in Karnovsky solution (1% glutaraldehyde in 0.2 M cacodylate buffer, pH 7.4). After fixation, the tissue was washed extensively in Veronal acetate buffer (90 mM, pH 6.0), stained with uranylmagnesium acetate (0.5%) in equilibration buffer (at 0 °C for 60 min), washed again, dehydrated, and embedded in paraffin. Then sections were rapidly cut into 0.5 mm cubes with a diamond knife and stained with uranyl acetate and lead citrate for viewing underneath a 200 CX TEM at 80 kV. The ultrastructure of TJs in tissues were evaluated by high magnification photography (11,500×).

Lipopolysaccharide assay

Blood was collected in a pyrogen-free, heparin-pretreated tube and centrifuged at 500 × *g* at 4 °C for 15 min. The LPS plasma ranges were assessed using a chromogenic kinetic limulus amebocyte lysate assay kit (Associates of Cape Cod, East Falmouth, MA, USA) following the manufacturer's instructions.

Western blot analysis

An equal amount of protein (30 μg/well) was extracted from each sample, separated by 6–10% sodium dodecyl sulfate polyacrylamide gel electrophoresis (SDS-PAGE), then transferred to a nitrocellulose membrane, and blocked for 1 h with a blocking buffer. The membrane was incubated with the appropriate primary antibody (Table 4) at 4 °C. The membrane was then washed three times with phosphate-buffered saline (PBS), then incubated with the appropriate secondary antibody (anti-rabbit IgG H&L). Finally, enhanced chemiluminescence (ECL) exposure was performed. The HP Scanjet XPA scanner was used to scan and save the exposure results, and the FR-980 bioelectrophoresis image analysis system was used to analyze the density integration of each band. Finally, the target western blot density integration and the interior reference blot density integration were calculated. These ratios were then used for quantification.

Immunofluorescence staining

Ileum tissue was embedded in OCT medium (Sakura Finetek, Torrance, CA, USA) and frozen rapidly in liquid nitrogen. Briefly, 8-μm thick cryostat slices were fixed in cold acetone for 15 min, rinsed three times for 5 min each in PBS, then permeabilized in 0.2% Triton X-100 (in PBS) for 5 min. After rinsing in PBS for 5 min, sections were blocked with 3% horse serum for 1 h at 25 °C, then incubated with either anti-occludin (1:100) or anti-ZO-1 (1:50) antibodies overnight at 4 °C. After rinsing three times for 6 min each in PBS, FITC goat anti-rabbit IgG (1:100) was added and incubated at room temperature for 30 min. The sections were then imaged with a laser scanning confocal microscope (OLYMPUS-FV10i, Olympus Corporation).

Quantitative reverse transcription polymerase chain reaction (RT-PCR)

Total RNA was extracted in accordance with the manufacturer's instructions (catalog number: E928KA9723, Sangon Biotech, Shanghai, China), and the RNA concentration was measured. Reverse transcription was carried out in accordance with manufacturer's instructions. The concentration of the

synthesized cDNA was measured and the cDNA was stored at –20 °C. Specific primers for amplifying target genes and endogenous actin (synthesized by Shanghai Shenggong Co., Shanghai, China) are provided in Table 5.

The two-step PCR procedure was as follows: one cycle of pre-denaturation at 95 ℃ for 10 sec, followed by 40 cycles of denaturation at 75 ℃ for 5 sec and amplification at 60 ℃ for 20 sec. The final products were confirmed using 1.5% agarose gel electrophoresis and melt curve analysis. Relative quantitative analysis was carried out using the double standard curve method. Calculation and analysis were carried out using the software program in the Rotor-Gene RG-3000 (Gene Co., Hong Kong, China).

Statistical analysis

Comparisons between groups were performed using one-way analysis of variation (ANOVA). Dunnet's multiple comparison post-tests were used to compare the means of different groups. The results are expressed as mean ± standard deviation. SPSS 24.0 (IBM, Armonk, NY, USA) and GraphPad Prism 7.0 (GraphPad Software, San Diego, CA, USA) were used for analysis, and $P < 0.05$ was considered statistically significant.

Results

UHPLC analysis of JHD

The results indicated that the chromatographic separation of all the analytes was satisfactory, and there was no interference in the solvent. The contents of naringin, paeoniflorin, puerarin, schisandrin a, atractylolide, and curcumin in JHD were 1.880%, 1.878%, 1.432%, 0.00718%, 0.00476%, and 0.00430%, respectively, while alisol 23b and tanshinone were not detectable (**Fig 1**).

Effect of JHD on liquid diet intake and body weight

Individual mice were weighed and food intake was recorded every 3 d. Both the total volume of liquid diets and average body weight in each experimental group were measured to compare the amount of alcohol intake and calories. There was no significant difference between the three groups ($P > 0.05$), suggesting that no effect from diet and alcohol consumption on the experimental results (**Fig 2**). One rat from the JHD group died due to improper intragastric irrigation during the first week of treatment.

JHD ameliorated alcohol-induced liver injury

Biomarkers of liver damage were analyzed and H&E staining was performed to determine the degree of chronic alcoholic liver injury. Steatosis was corroborated by biochemical measurement of the levels of hepatic TG. Chronic daily alcohol consumption caused liver injury based on all our outcome measures. Analysis of serum AST, ALT, and AKP showed that enzyme levels in the model group were significantly higher than the control group, whereas JHD pretreatment resulted in significantly decreased expression ($P < 0.05$; **Fig 3a–c**). The liver H&E results were consistent with the significant changes in the

levels of hepatic TG. JHD significantly decreased the TG content in the liver ($P < 0.05$; **Fig 3d**). H&E staining revealed extensive steatosis with inflammatory infiltration in ethanol-fed rats. Most macrovesicular steatosis was around the vein, progressively extending to the mid-zonal and periportal regions. Some ballooned hepatocytes showed watery and edematous, wispy, rarefied cytoplasm. When these changes were quantified using histological liver damage index scores, the scores of alcohol-fed rats were significantly higher ($P < 0.01$) than control rats. By contrast, pathological changes and damage index scores were significantly improved in the JHD-treated group (**Fig 3e–g**).

JHD ameliorated gut-leakage in ALD

We next compared LPS translocation and ileum morphology to assess intestinal epithelial permeability after long-term ethanol intake and JHD administration. The level of portal vein blood LPS, measured 3.5 h after a single oral dose of 10 mg/kg LPS, in the model group was significantly higher than in the control group ($P < 0.05$). JHD treatment reduced LPS uptake levels ($P < 0.05$; **Fig 4a**).

The ileum H&E staining and "Chiu" score showed that long-term ethanol stimulation significantly increased the microvilli of epithelial cell injury and caused mild inflammatory cell infiltration. JHD pretreatment prevented these abnormalities and restored their morphology. In addition, ileum pathological scores of the JHD-treated group were significantly improved (**Fig 4b,c**). TEM images of ileum epithelial cells in the model group revealed that brush border microvilli at the apical surface became more loosely packed and highly variable in length compared with the control group. Moreover, the ultrastructure of intercellular junctions, especially TJs, were disrupted in ethanol-fed rats. In contrast, ileum epithelial cells from JHD-treated rats showed slightly more degeneration, with occasional nuclear pyknosis, improved focal loosely packed microvilli, and integrated connection structures of TJs (**Fig 4d**).

JHD restored intestinal tight junctions in ALD

We next explored the effects of JHD treatment on TJ alterations in rats administered a Lieber-DeCarli ethanol liquid diet. Protein expression analysis demonstrated that JHD-treatment maintained ZO-1 and occludin expression levels in chronic alcoholic livers in JHD-treated rats. JHD could upregulate expression of ZO-1 and occludin protein in the ileum ($P < 0.01$, **Fig 5a,b**). However, the mRNA expression levels for these two genes were markedly lower in the model group compared to the control group. JHD treatment significantly prevented drastic losses in the expression of these two mRNAs ($P < 0.05$ or $P < 0.01$, **Fig 5c**).

Confocal laser scanning micrographs of immunofluorescence staining showed that the cytoplasmic plaque protein ZO-1 was predominantly expressed in the cytosolic fraction, and the transmembrane TJ protein occludin was primarily expressed in the membrane fraction. JHD administration clearly reduced the loss of both ZO-1 and occludin in ethanol-treated rats (**Fig 5d**).

JHD downregulated phosphorylation of MLC in the ileum

MLC kinase (MLCK)-mediated MLC phosphorylation is a key regulator of TJ permeability. We measured MLCK and p-MLC levels using western blotting to investigate how these enzymes modulate the TJ proteins during paracellular permeability changes. Long-term ethanol intake slightly reduced the expression of MLCK, although this difference was not significant. The levels of p-MLC in ileum, however, were substantially enhanced ($P < 0.01$). JHD could downregulate ethanol-induced MLC phosphorylation ($P < 0.05$; **Fig 6**).

Discussion

In the current study, we investigated the effect of JHD treatment on amelioration of ALD in rats and probed the underlying mechanisms. We used the traditional Lieber-DeCarli model, which is an easy, accurate, and dependable model to identify pathogenesis of the early stages of ALD [19]. The Lieber-DeCarli diet induced extreme liver injury, as evidenced by the significant increases in plasma ALT, AST, AKP, and hepatic TG, as well as by the pathological changes in the liver (e.g., steatosis and inflammation), which were remarkably ameliorated following JHD treatment.

Our prior research demonstrated that JHD alleviates alcohol-induced liver injury [18]. This study preliminarily confirmed that the levels of plasma LPS in the model group were significantly higher than the control group. Ileum pathology and electron microscopy revealed intestinal epithelial cell disorganization with abnormal morphology in alcohol-exposed rats. Here, we showed that JHD can significantly reduce the levels of serum LPS. Moreover, inflammation of the ileum was alleviated as evidenced by H&E staining and electron microscopy. Our outcomes indicated that LPS affects ALD occurrence, and there is a positive correlation between the ileum and liver.

Dysbiosis of the intestinal barrier is closely related to the onset and progression of ALD [22]. The intestinal barrier can not only selectively permit the absorption of nutrients, but also maintains a robust defense against intestinal endotoxins, antigens, and microorganisms from entering the blood circulation [14]. The physical barrier is provided by TJs between epithelia and is the most essential section of the intestinal barrier [23]. Occludin is a key TJ protein and its expression levels determine properties of the intestinal tissue barrier [24]. ZO-1 is a peripheral membrane protein which is crucial for TJ assembly and maintenance, due in part to protein-protein interactions with occludin [25]. We also demonstrate that the protein and mRNA levels of ZO-1 and occludin were remarkably increased by JHD treatment, returning to basal levels consistent with no alcohol exposure. In addition, immunofluorescence results suggest that JHD can considerably enhance the localized sparseness of microvilli on the surface of the ileum mucosa, and irregular arrangement and uneven distribution of ZO-1 in the ileum. This suggests that JHD can enhance intestinal permeability by improving TJs in intestinal epithelial cells.

Based on the above results, we tried to determine how JHD treatment induced upregulation of ZO-1 and occludin and enhanced the stability of epithelial cell TJs. MLCK-mediated MLC phosphorylation and myosin contractility are essential for the regulation of physiological and pathological functions of the intestinal barrier [26]. A previous study confirmed that epithelial cell lines with altered MLC

phosphorylation were unable to significantly strengthen barrier function, suggesting that TJ assembly was disrupted [27]. In addition, a recent study showed that MLCK, especially p-MLC, induces contraction of the prejunctional actomyosin ring, indicating that it is a key regulator of TJ permeability [28]. *In vivo*, p-MLC causes a subtle change in ZO-1 localization, and immunofluorescence imaging confirmed decreased ZO-1 staining [29]. *In vitro*, p-MLC elevates TJ permeability, redistributes ZO-1 and occludin, and alters morphology and biochemical function [30]. We detected MLCK and p-MLC protein expression in ileum; however, the expression of MCLK protein did not differ significantly between the control and model groups ($P > 0.05$). However, the level of p-MLC protein in the model group was significantly higher than the control group. After JHD treatment, p-MLC levels decreased significantly. This suggests that alcohol stimulation leads to MLC phosphorylation, inflicting injury to the physical barrier of the ileum. JHD can decrease the level of p-MLC, thereby regulating TJs and enhancing intestinal permeability.

This study demonstrated that JHD can protect against ALD and ameliorate hepatic steatosis and hepatic inflammation. In addition, JHD protected against ALD is achieved at multiple levels within the ileum, including decreasing in portal vein LPS levels, regulating intestinal tight junctions via inhibiting p-MLC, and enhancing intestinal barrier function (Fig. 7). These results demonstrate that the protective actions of JHD in the ileum critically contribute to its beneficial effect against alcoholic steatohepatitis. However, further studies are needed to clarify the mechanism by which JHD affects ALD in rats.

Conclusions

The above results suggest that JHD has potential value for the prevention and treatment of ALD in rats, and its mechanism may be closely related to its effect on protecting intestinal barrier function and attenuating gut leakiness.

Abbreviations

JHD, Jianpi huoxue decoction; ALD, alcoholic liver disease; HCC, hepatocellular carcinoma; LPS, lipopolysaccharide; TJs, tight junctions; MLCK, myosin light chain kinase; p-MLC, phosphorylated myosin light chain; ALT, alanine aminotransferase; AST, aspartate aminotransferase; AKP, alkaline phosphatase; TG, triglyceride; ZO-1, zonula occludens 1; TCM, traditional Chinese medicine

Declarations

Acknowledgements

We thank Siting Gao for providing techinical assistance.

Author contributious

Qin Feng, Yiyang Hu designed this study. Xin Wang, Dongsheng Yao, Qilin Fu, Lin Xu, and Dongming Yao performed the experiments. Yu Zhao, Jinghua Peng, Qin Feng, Qilin Fu, Yiyang Hu analysed the data. Qin

Feng, Xin Wang, Lin Xu wrote the manuscript. Qin Feng revised the manuscript. All authors critically participated in the discussion and commented on the manuscript.

Financial support

This work was supported by National Science Foundation of China (No.30801536, to Q. F.)

Availability of data and materials

The supporting materials can be obtained upon request via email to the corresponding author.

Ethics and consent to participate

All of the experiments involving animals were in accordance with the guidelines of the Institutional Animal Care and Use Committee of Shanghai University of Traditional Chinese Medicine.All animal testing protocols were approved by the Animal Experimental Ethics Committee of Shanghai University of Traditional Chinese Medicine.

Conflict of interest

The authors declare no potential conflicts of interest.

References

1. Avila MA, Dufour JF, Gerbes AL, Zoulim F, Bataller R, Burra P, Cortez-Pinto H, Gao B, Gilmore I, Mathurin P *et al*: **Recent advances in alcohol-related liver disease (ALD): summary of a Gut round table meeting**. *Gut* 2020, **69**(4):764–780.
2. Teschke R: **Alcoholic steatohepatitis (ASH) and alcoholic hepatitis (AH): cascade of events, clinical aspects, and pharmacotherapy options**. *Expert Opin Pharmacother* 2018, **19**(8):779–793.
3. Thursz M, Kamath PS, Mathurin P, Szabo G, Shah VH: **Alcohol-related liver disease: Areas of consensus, unmet needs and opportunities for further study**. *J Hepatol* 2019, **70**(3):521–530.
4. Bukong TN, Cho Y, Iracheta-Vellve A, Saha B, Lowe P, Adejumo A, Furi I, Ambade A, Gyongyosi B, Catalano D *et al*: **Abnormal neutrophil traps and impaired efferocytosis contribute to liver injury and sepsis severity after binge alcohol use**. *J Hepatol* 2018, **69**(5):1145–1154.
5. Ge X, Leung TM, Arriazu E, Lu Y, Urtasun R, Christensen B, Fiel MI, Mochida S, Sorensen ES, Nieto N: **Osteopontin binding to lipopolysaccharide lowers tumor necrosis factor-alpha and prevents early alcohol-induced liver injury in mice**. *Hepatology* 2014, **59**(4):1600–1616.
6. Liang S, Zhong Z, Kim SY, Uchiyama R, Roh YS, Matsushita H, Gottlieb RA, Seki E: **Murine macrophage autophagy protects against alcohol-induced liver injury by degrading interferon regulatory factor 1 (IRF1) and removing damaged mitochondria**. *Journal of Biological Chemistry* 2019, **294**(33):12359–12369.

7. Mathurin P, Deng QG, Keshavarzian A, Choudhary S, Holmes EW, Tsukamoto H: **Exacerbation of alcoholic liver injury by enteral endotoxin in rats**. *Hepatology* 2000, **32**(5):1008–1017.
8. Enomoto N, Ikejima K, Yamashina S, Hirose M, Shimizu H, Kitamura T, Takei Y, Sato N, Thurman RG: **Kupffer cell sensitization by alcohol involves increased permeability to gut-derived endotoxin**. *Alcohol Clin Exp Res* 2001, **26**(6):51S-54S.
9. Wang Y, Tong J, Chang B, Wang B, Zhang D, Wang B: **Effects of alcohol on intestinal epithelial barrier permeability and expression of tight junction-associated proteins**. *Mol Med Rep* 2014, **9**(6):2352–2356.
10. Purohit V, Bode JC, Bode C, Brenner DA, Choudhry MA, Hamilton F, Kang YJ, Keshavarzian A, Rao R, Sartor RB *et al*: **Alcohol, intestinal bacterial growth, intestinal permeability to endotoxin, and medical consequences: summary of a symposium**. *Alcohol* 2008, **42**(5):349–361.
11. Tang Y, Banan A, Forsyth CB, Fields JZ, Lau CK, Zhang LJ, Keshavarzian A: **Effect of alcohol on miR-212 expression in intestinal epithelial cells and its potential role in alcoholic liver disease**. *Alcohol Clin Exp Res* 2008, **32**(2):355–364.
12. Van Spaendonk H, Ceuleers H, Witters L, Patteet E, Joossens J, Augustyns K, Lambeir A-M, De Meester I, De Man JG, De Winter BY: **Regulation of intestinal permeability: The role of proteases**. *World Journal of Gastroenterology* 2017, **23**(12):2106.
13. Suzuki T: **Regulation of intestinal epithelial permeability by tight junctions**. *Cellular and Molecular Life Sciences* 2012, **70**(4):631–659.
14. Groschwitz KR, Hogan SP: **Intestinal barrier function: molecular regulation and disease pathogenesis**. *J Allergy Clin Immunol* 2009, **124**(1):3–20; quiz 21–22.
15. Buckley A, Turner JR: **Cell Biology of Tight Junction Barrier Regulation and Mucosal Disease**. *Cold Spring Harbor Perspectives in Biology* 2018, **10**(1):a029314.
16. Keshavarzian A, Holmes EW, Patel M, Iber F, Fields JZ, S. P: **Leaky gut in alcoholic cirrhosis: a possible mechanism for alcohol-induced liver damage**. 1999, **94**(**1**):200–207.
17. Ulluwishewa D, Anderson RC, McNabb WC, Moughan PJ, Wells JM, Roy NC: **Regulation of tight junction permeability by intestinal bacteria and dietary components**. *J Nutr* 2011, **141**(5):769–776.
18. Z.H. Fang, Y.Y. Hu, J.W. Cui, X. Lu, X.N. Wang, J.H. Peng, Feng. Q: **Relationship between alcoholic liver injury and endotoxin leakage from gut and intervention effect of jianpi liqi huoxue decoction**. *Zhongguo Zhong Xi Yi Jie He Za Zhi* 2006, **269**(9):813–817.
19. Guo F, Zheng K, Benede-Ubieto R, Cubero FJ, Nevzorova YA: **The Lieber-DeCarli Diet-A Flagship Model for Experimental Alcoholic Liver Disease**. *Alcohol Clin Exp Res* 2018, **42**(10):1828–1840.
20. Yang X, He F, Zhang Y, Xue J, Li K, Zhang X, Zhu L, Wang Z, Wang H, Yang S: **Inulin Ameliorates Alcoholic Liver Disease via Suppressing LPS-TLR4-Mpsi Axis and Modulating Gut Microbiota in Mice**. *Alcohol Clin Exp Res* 2019, **43**(3):411–424.
21. Chiu CJ, McArdle AH, Brown R, Scott HJ, FN G: **Intestinal mucosal lesion in low-flow states. I. A morphological, hemodynamic, and metabolic reappraisal**. *Arch Surg* 1970, **101**:478–483.

22. Maccioni L, Gao B, Leclercq S, Pirlot B, Horsmans Y, De Timary P, Leclercq I, Fouts D, Schnabl B, Stärkel P: **Intestinal permeability, microbial translocation, changes in duodenal and fecal microbiota, and their associations with alcoholic liver disease progression in humans**. *Gut Microbes* 2020, **12**(1):1782157.
23. Camara-Lemarroy CR, Metz L, Meddings JB, Sharkey KA, Wee Yong V: **The intestinal barrier in multiple sclerosis: implications for pathophysiology and therapeutics**. *Brain* 2018, **141**(7):1900–1916.
24. Harhaj NS, Antonetti DA: **Regulation of tight junctions and loss of barrier function in pathophysiology**. *Int J Biochem Cell Biol* 2004, **36**(7):1206–1237.
25. Turner JR: **Intestinal mucosal barrier function in health and disease**. *Nat Rev Immunol* 2009, **9**(11):799–809.
26. Shen Q, Rigor RR, Pivetti CD, Wu MH, Yuan SY: **Myosin light chain kinase in microvascular endothelial barrier function**. *Cardiovascular Research* 2010, **87**(2):272–280.
27. Gandhi S, Lorimer DD, de Lanerolle P: **Expression of a mutant myosin light chain that cannot be phosphorylated increases paracellular permeability**. *Am J Physiol* 1997, **272**(5):F214-F221.
28. Cunningham KE, Turner JR: **Myosin light chain kinase: pulling the strings of epithelial tight junction function**. *Ann N Y Acad Sci* 2012, **1258**:34–42.
29. Clayburgh DR, Barrett TA, Tang Y, Meddings JB, Van Eldik LJ, Watterson DM, Clarke LL, Mrsny RJ, Turner JR: **Epithelial myosin light chain kinase-dependent barrier dysfunction mediates T cell activation-induced diarrhea in vivo**. *J Clin Invest* 2005, **115**(10):2702–2715.
30. Shen L, Black ED, Witkowski ED, Lencer WI, Guerriero V, Schneeberger EE, Turner JR: **Myosin light chain phosphorylation regulates barrier function by remodeling tight junction structure**. *J Cell Sci* 2006, **119**(Pt 10):2095–2106.

Tables

Table . Components in the formula of JHD

Chinese name	Botanical name	Family name	Production place	Processing method
Jiang Huang	*Curuma longa L.*	Zingiberaceae	Fujian Province China	Ethanol extraction
Zhi Qiao	*Citrus aurantium L.*	Rutaceae	Jiangxi Province China	Ethanol extraction
Bai Zhu	*Altractylodes macrocephala Koidz.*	Asteraceae	Zhejiang Province, China	Ethanol extraction
Wu Wei Zi	*Schisandra chinensis (turcz.) Baill.*	Magnoliaceae	Liaoning Province, China	Ethanol extraction
Dan Shen	*Salvia miltiorrhiza Bge.*	Labiatae	Shandong Province, China	Water extraction
Bai Shao	*Paeonia lzctiilora pall.*	Ranunculaceae	Anhui Province China	Water extraction
Ze Xie	*Alisma orientalis (sam.) Juzep.*	Alismataceae	Sichuan Province China	Water extraction
Ge Gen	*Pueraria lobata (willd.) Ohwi.*	Leguminosae	Anhui Province China	Water extraction

Table . Lieber-DeCarli diet composition

Ingredient	Grams/Liter of diet
Casein	41.4
L-Cystine	0.5
DL-Methionine	0.3
Corn Oil	8.5
Olive Oil	28.4
Safflower	2.7
Maltose Dextrin	25.6
Cellulose	10.0
Salt Mix	8.75
Vitamin Mix	2.5
Choline Bitartrate	0.53
Xanthan Gum	3.0
95% ethanol	67.3 ml

Table . non-alcohol diet composition

Ingredient	Grams/Liter of diet
Casein	41.4
L-Cystine	0.5
DL-Methionine	0.3
Corn Oil	8.5
Olive Oil	28.4
Safflower	2.7
Maltose Dextrin	115.2
Cellulose	10.0
Salt Mix	8.75
Vitamin Mix	2.5
Choline Bitartrate	0.53
Xanthan Gum	3.0

Table . Antibodies for western blotting and immunofluorescence staining

Antibody	Manufacturer catalog	Species	Western blotting	Immunofluorescence staining
ZO-1	santa cruz biotechnology, SC-10804	Rabbit	1: 100	1: 50
Occludin	Abcam, ab31721	Rabbit	1: 250	1:100
MLCK	EPITOMICS, 2095-1	Rabbit	1: 1000	
p-MLCK	Cell signaling, #3671	Rabbit	1: 1000	
-tublin	EPITOMICS, 2251-1	Rabbit	1: 1000	
FITC	santa cruz biotechnology, SC-2012	Goat		1100
Anti-rabbit IgG H&L	Biotech, MR-G100	Goat		15000

Table . DNA sequences of mouse primers used for real-time RT-PCR

Target gene	Sequence	Product length, bp
ZO-1	5'-CAC CAG ACC ATG CTT CAG TGA GA-3'(F) 5'-GTT GCA TGG CTG TTC ACA GGA-3'(R)	151bp
Occludin	5'-GTC TTG GGA GCC TTG ACA TCT TG-3'(F) 5'- GCA TTG GTC GAA CGT GCA TC-3'(R)	174bp
β-actin	5'-TGA CGA GGC CCA GAG CAA GA-3'(F) 5'-ATG GGC ACA GTG TGG GTG AC-3'(R)	331bp

Figures

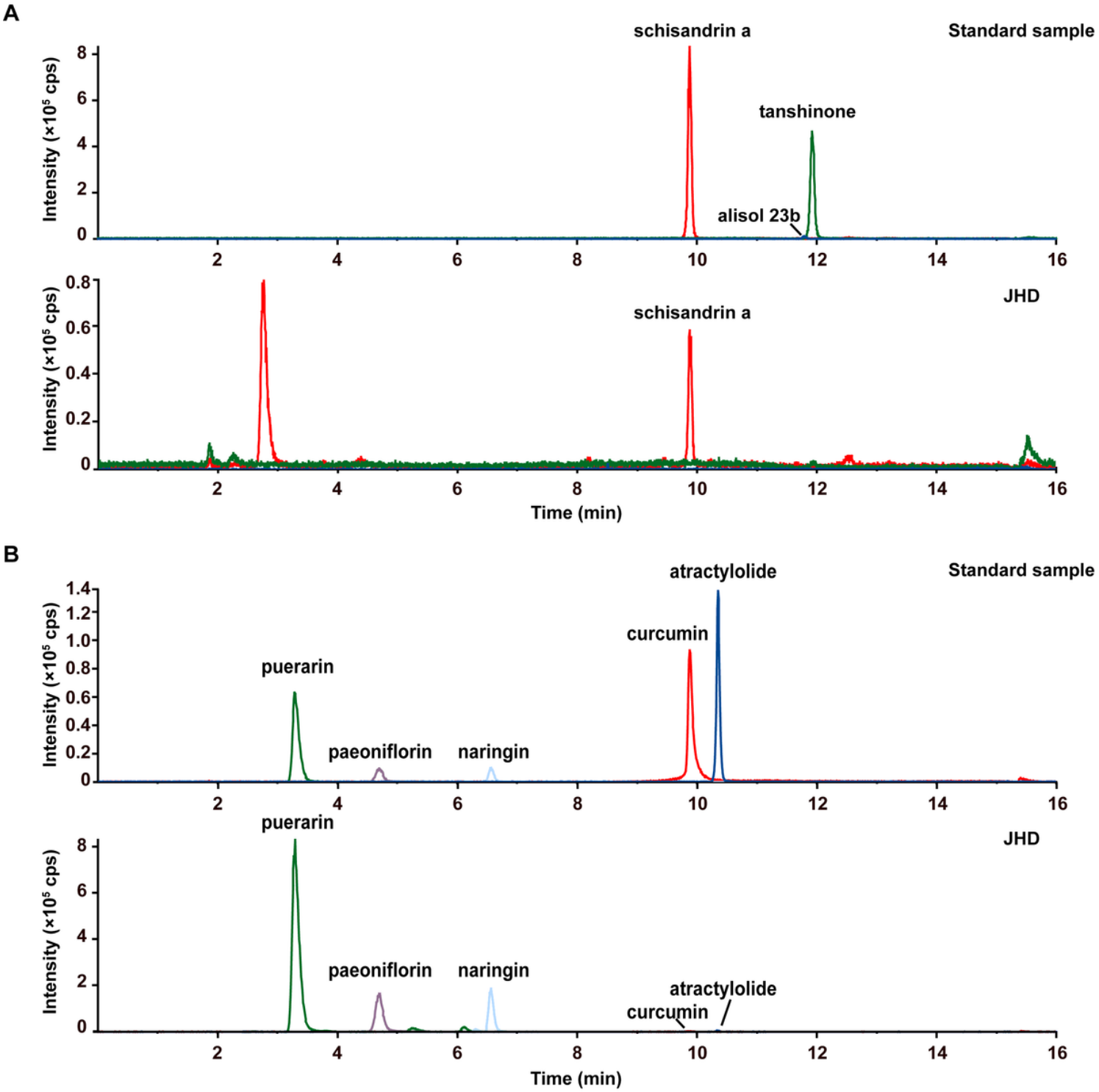

Figure 1

UHPLC chromatograms of the JHD. (A) and (B): Standard sample (the upper) and JHD (the lower). (A) Schisandrin a, alisol 23b and tanshinone were analyzed in ESI+ mode. Alisol 23b and tanshinone were not detectable. (B) Puerarin, paeoniflorin, naringin, curcumin and atractylolide were analyzed in ESI- mode.

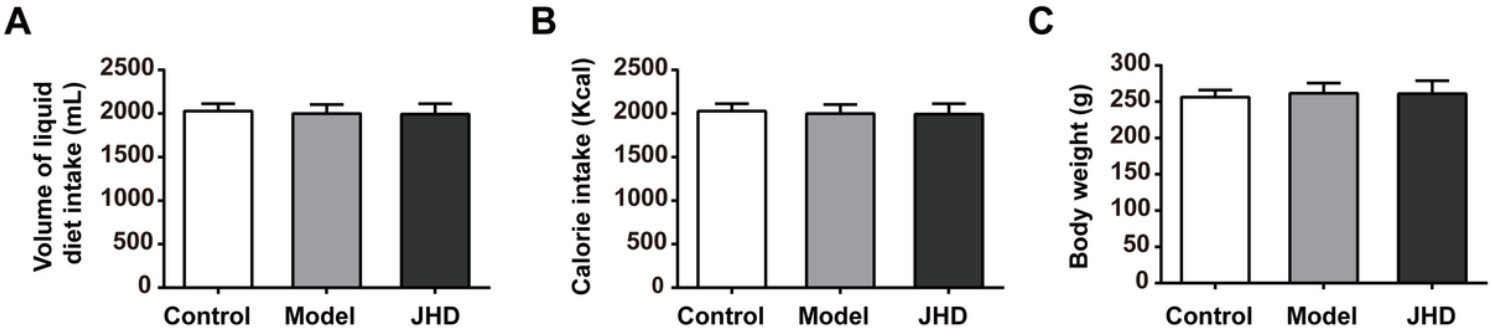

Figure 2

General conditions of the rats in each group. (A) Volume of liquid diet intake. (B) Calorie intake. (C) Body weight. Data are represented as means±SD. Control, n=10; Model, n=10; JHD, n=9.

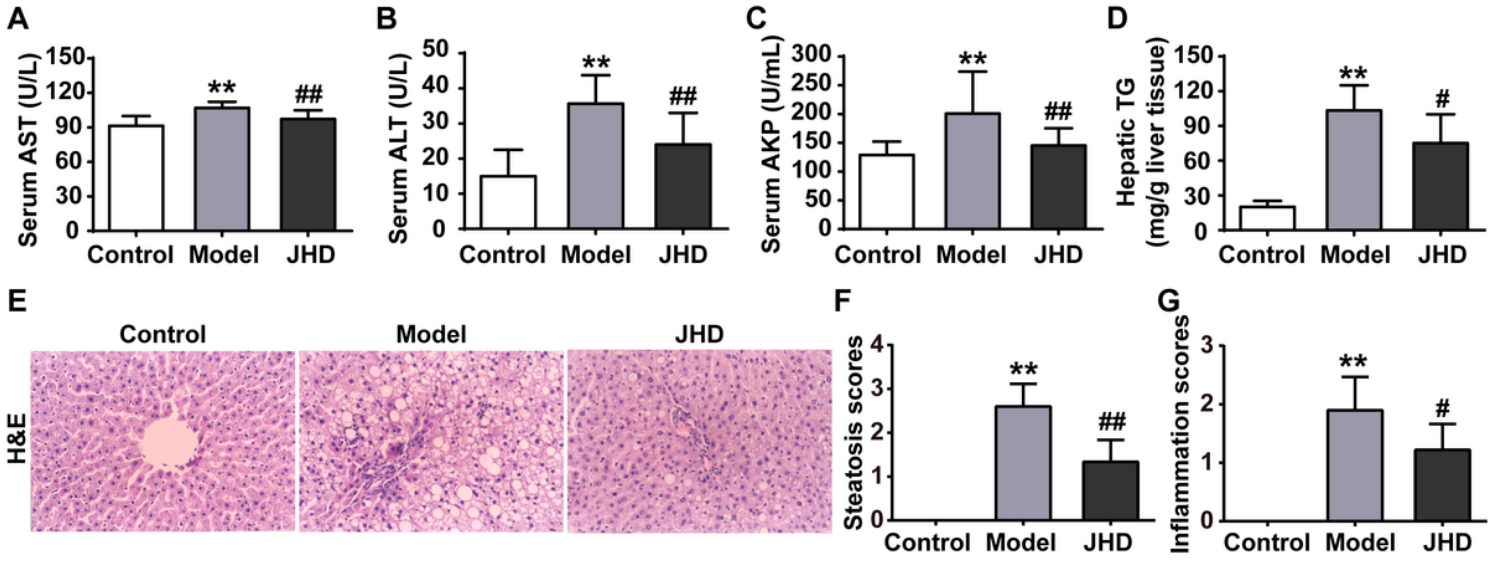

Figure 3

JHD reduces liver dysfunction and improves histopathological changes in the liver of ALD rats. (A-D) Serologic indicators of liver function. (A) Aspartate aminotransferase levels (AST). (B) Alanine aminotransferase levels (ALT). (C) Alkaline phosphatase levels (AKP). (D) Hepatic TG. (E) Representative images of H&E staining, (200×). (F) Steatosis scores. (G) Inflammation scores. Data are represented as means±SD. Control, n=10; Model, n=10; JHD, n=9. * P 0.05, ** P 0.01 vs. the control group; # P 0.05, ## P 0.01 vs. the model group.

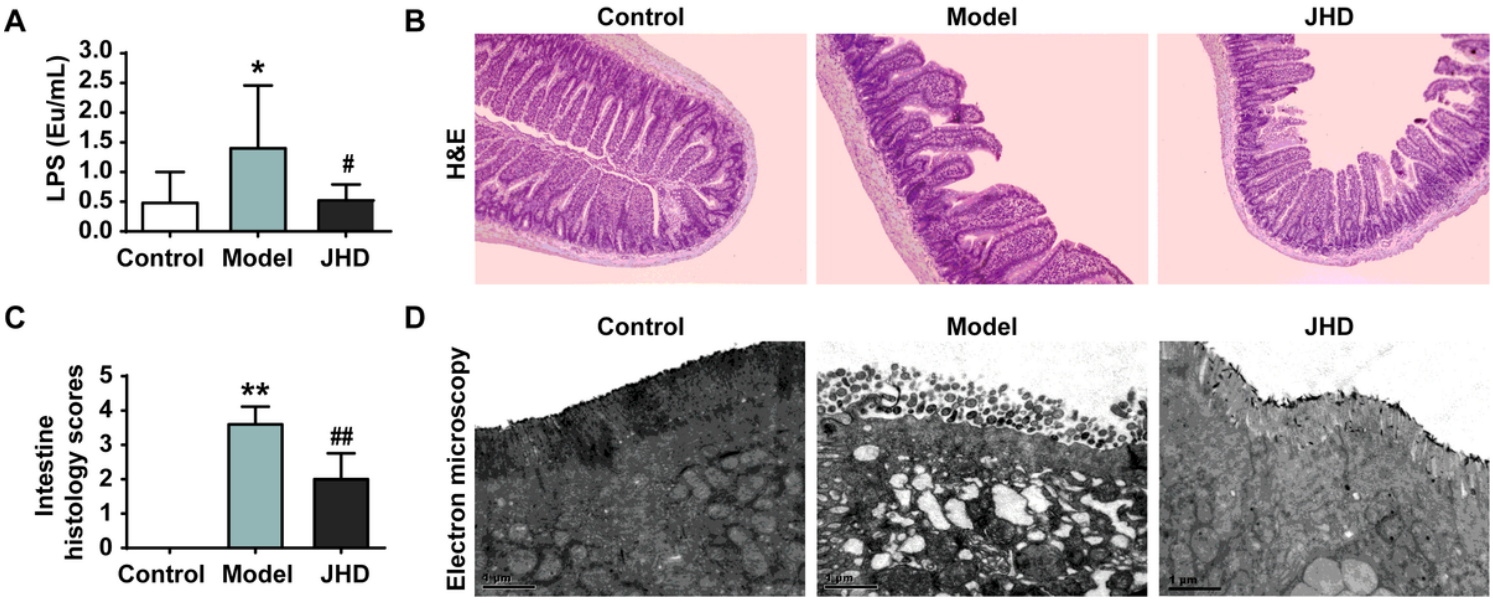

Figure 4

JHD significantly decreases the plasma endotoxin level by improving intestinal hyper-permeability in ALD rats. (A) The plasma endotoxin levels in portal vein. (B) Representative images of the intestine with H&E staining. Original magnification, (200×). (C) Intestine inflammation scores. (D) Transmission electron micrographs images of intestinal epithelial cells. Original magnification, (11500×). Data are represented as means±SD. Control, n=10; Model, n=10; JHD, n=9. * P 0.05, ** P 0.01 vs. the control group; # P 0.05, ## P 0.01 vs. the model group.

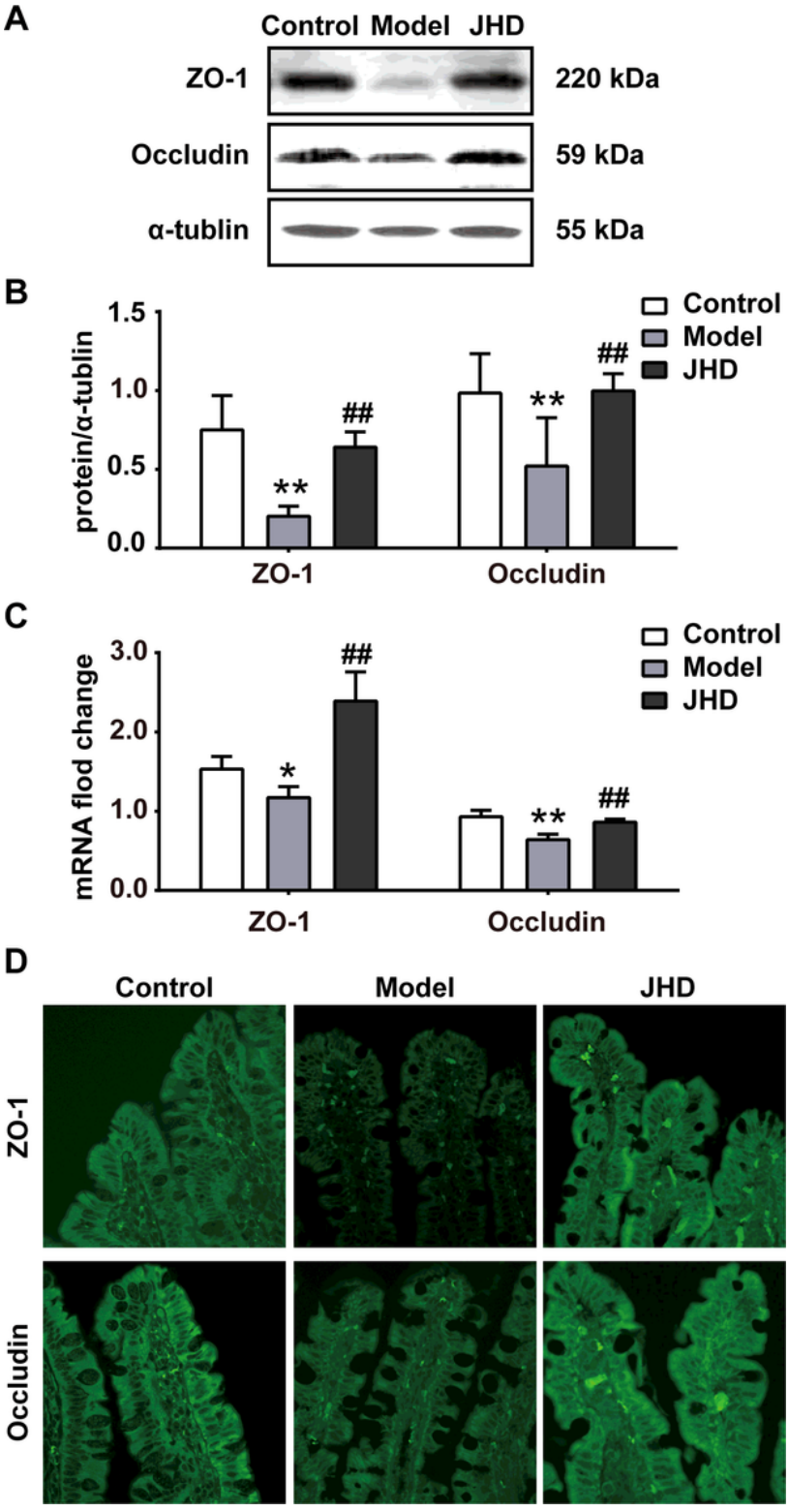

Figure 5

JHD inhibits the ethanol-induced intestinal barrier dysfunction by regulating the intestinal epithelial tight junction. (A-B) Western blot analysis of ZO-1 and occludin protein expression level in intestine, and semi-quantitative analysis was performed with ImageJ software. (C) Gene expression analysis (RT–PCR) of ZO-1 and occludin in intestine. (D) Confocal images representing immunofluorescence staining for ZO-1 and occludin in cryosections of intestine biopsies. Data are represented as means±SD. Control, n=10;

Model, n=10; JHD, n=9. * P 0.05, ** P 0.01 vs. the control group; # P 0.05, ## P 0.01 vs. the model group.

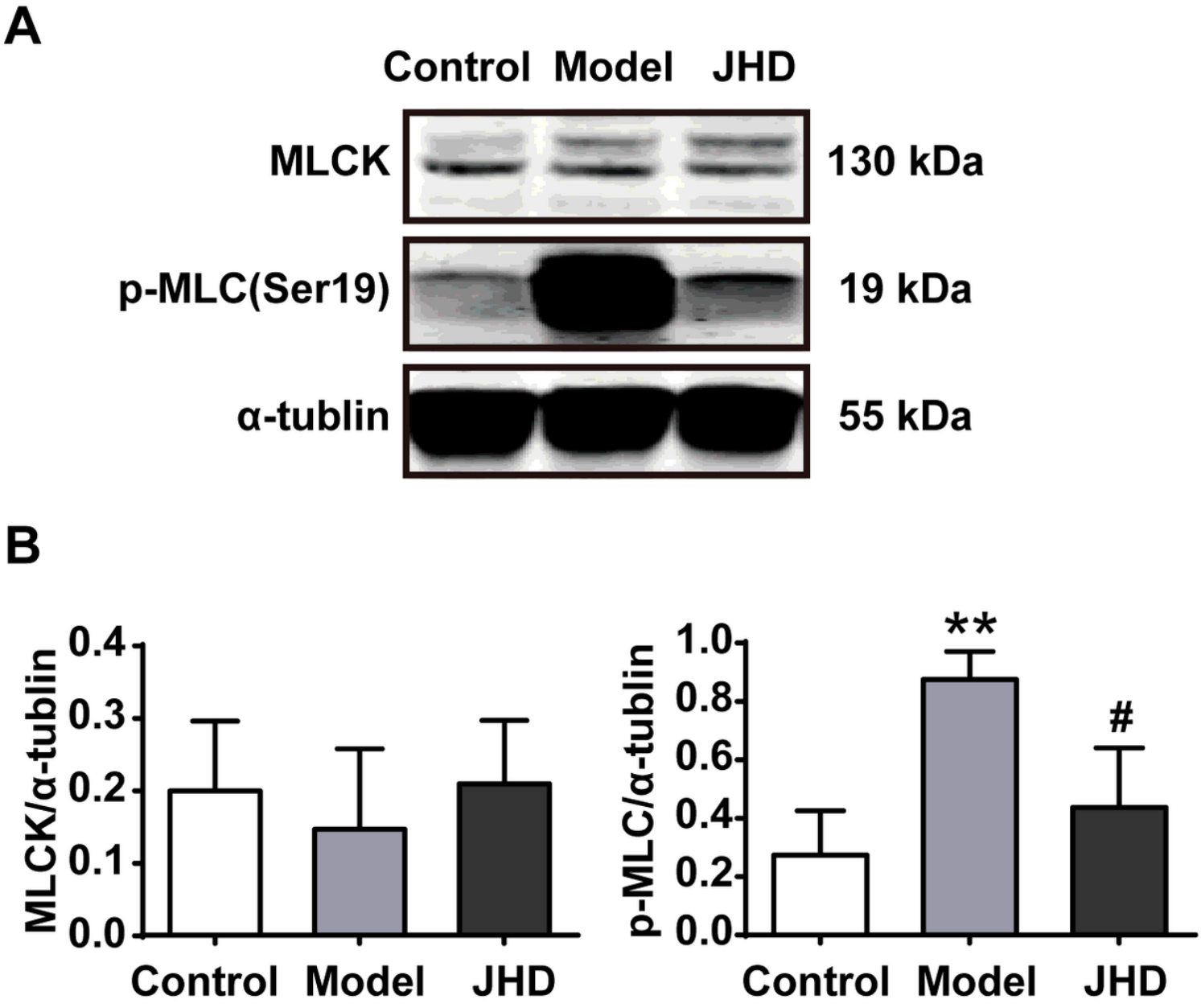

Figure 6

JHD prevents intestinal mucosal mechanical barrier associated with reducing ethanol-induced phosphorylation of myosin light chain. (A)Western blot analysis of MLCK and p-MLC protein expression level in intestine. (B) The gray-level score indicates the immunoblotting histogram for MLCK and p-MLC, performed with ImageJ software, expressed in arbitrary units. Data are represented as means±SD. Control, n=3; Model, n=3; JHD, n=3. * P 0.05, ** P 0.01 vs. the control group; # P 0.05, ## P 0.01 vs. the model group.

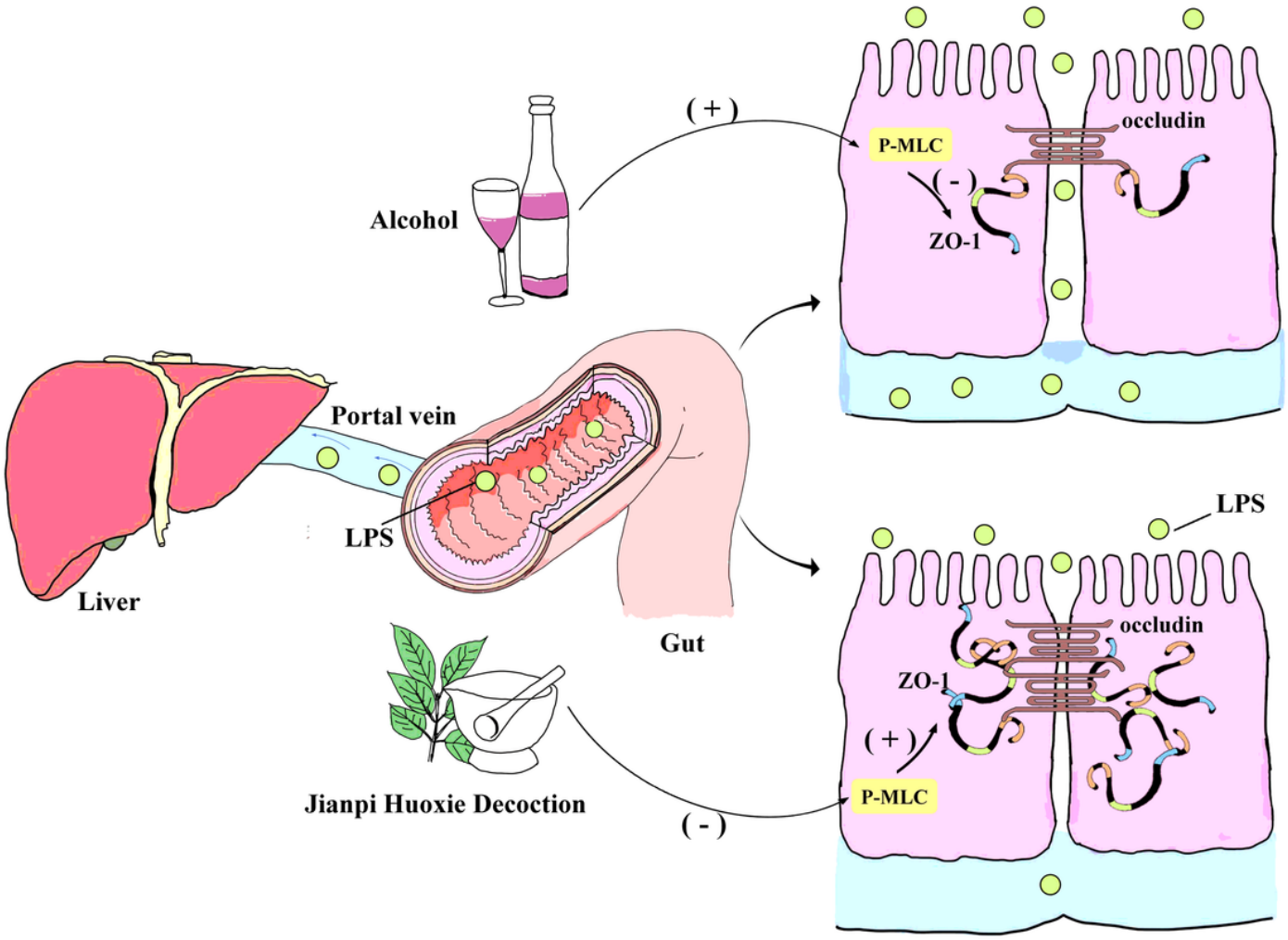

Figure 7

Patterns of effectiveness of JHD for the treatment of ALD by regulating intestinal tight junctions via inhibiting myosin light chain phosphorylation and protecting intestinal barrier function.

Supplementary Files

This is a list of supplementary files associated with this preprint. Click to download.

- Supplementarymetarials.docx